

Search for invisible decays of the Λ baryon

M. Ablikim,¹ M. N. Achasov,^{10,b} P. Adlarson,⁶⁶ S. Ahmed,¹⁴ M. Albrecht,⁴ R. Aliberti,²⁷ A. Amoroso,^{65a,65c} M. R. An,³¹ Q. An,^{62,48} X. H. Bai,⁵⁶ Y. Bai,⁴⁷ O. Bakina,²⁸ R. Baldini Ferroli,^{22a} I. Balossino,^{23a} Y. Ban,^{37,h} K. Begzsuren,²⁵ N. Berger,²⁷ M. Bertani,^{22a} D. Bettoni,^{23a} F. Bianchi,^{65a,65c} J. Bloms,⁵⁹ A. Bortone,^{65a,65c} I. Boyko,²⁸ R. A. Briere,⁵ H. Cai,⁶⁷ X. Cai,^{1,48} A. Calcaterra,^{22a} G. F. Cao,^{1,53} N. Cao,^{1,53} S. A. Cetin,^{52a} J. F. Chang,^{1,48} W. L. Chang,^{1,53} G. Chelkov,^{28,a} D. Y. Chen,⁶ G. Chen,¹ H. S. Chen,^{1,53} M. L. Chen,^{1,48} S. J. Chen,³⁴ X. R. Chen,²⁴ Y. B. Chen,^{1,48} Z. J. Chen,^{19,i} W. S. Cheng,^{65c} G. Cibinetto,^{23a} F. Cossio,^{65c} X. F. Cui,³⁵ H. L. Dai,^{1,48} X. C. Dai,^{1,53} A. Dbeyssi,¹⁴ R. E. de Boer,⁴ D. Dedovich,²⁸ Z. Y. Deng,¹ A. Denig,²⁷ I. Denysenko,²⁸ M. Destefanis,^{65a,65c} F. De Mori,^{65a,65c} Y. Ding,³² C. Dong,³⁵ J. Dong,^{1,48} L. Y. Dong,^{1,53} M. Y. Dong,^{1,48,53} X. Dong,⁶⁷ S. X. Du,⁷⁰ Y. L. Fan,⁶⁷ J. Fang,^{1,48} S. S. Fang,^{1,53} Y. Fang,¹ R. Farinelli,^{23a} L. Fava,^{65b,65c} F. Feldbauer,⁴ G. Felici,^{22a} C. Q. Feng,^{62,48} J. H. Feng,⁴⁹ M. Fritsch,⁴ C. D. Fu,¹ Y. Gao,⁶³ Y. Gao,^{62,48} Y. Gao,^{37,h} Y. G. Gao,⁶ I. Garzia,^{23a,23b} P. T. Ge,⁶⁷ C. Geng,⁴⁹ E. M. Gersabeck,⁵⁷ A. Gilman,⁶⁰ K. Goetzen,¹¹ L. Gong,³² W. X. Gong,^{1,48} W. Gradl,²⁷ M. Greco,^{65a,65c} L. M. Gu,³⁴ M. H. Gu,^{1,48} C. Y. Guan,^{1,53} A. Q. Guo,²¹ L. B. Guo,³³ R. P. Guo,³⁹ Y. P. Guo,^{9,f} A. Guskov,^{28,a} T. T. Han,⁴⁰ W. Y. Han,³¹ X. Q. Hao,¹⁵ F. A. Harris,⁵⁵ K. L. He,^{1,53} F. H. Heinsius,⁴ C. H. Heinz,²⁷ Y. K. Heng,^{1,48,53} C. Herold,⁵⁰ M. Himmelreich,^{11,d} T. Holtmann,⁴ G. Y. Hou,^{1,53} Y. R. Hou,⁵³ Z. L. Hou,¹ H. M. Hu,^{1,53} J. F. Hu,^{46,j} T. Hu,^{1,48,53} Y. Hu,¹ G. S. Huang,^{62,48} L. Q. Huang,⁶³ X. T. Huang,⁴⁰ Y. P. Huang,¹ Z. Huang,^{37,h} T. Hussain,⁶⁴ N. Hüsken,^{21,27} W. Ikegami Andersson,⁶⁶ W. Imoehl,²¹ M. Irshad,^{62,48} S. Jaeger,⁴ S. Janchiv,²⁵ Q. Ji,¹ Q. P. Ji,¹⁵ X. B. Ji,^{1,53} X. L. Ji,^{1,48} Y. Y. Ji,⁴⁰ H. B. Jiang,⁴⁰ X. S. Jiang,^{1,48,53} J. B. Jiao,⁴⁰ Z. Jiao,¹⁷ S. Jin,³⁴ Y. Jin,⁵⁶ M. Q. Jing,^{1,53} T. Johansson,⁶⁶ N. Kalantar-Nayestanaki,⁵⁴ X. S. Kang,³² R. Kappert,⁵⁴ M. Kavatsyuk,⁵⁴ B. C. Ke,^{42,i} I. K. Keshk,⁴ A. Khoukaz,⁵⁹ P. Kiese,²⁷ R. Kiuchi,¹ R. Kliemt,¹¹ L. Koch,²⁹ O. B. Kolcu,^{52a} B. Kopf,⁴ M. Kuemmel,⁴ M. Kuessner,⁴ A. Kupsc,⁶⁶ M. G. Kurth,^{1,53} W. Kühn,²⁹ J. J. Lane,⁵⁷ J. S. Lange,²⁹ P. Larin,¹⁴ A. Lavania,²⁰ L. Lavezzi,^{65a,65c} Z. H. Lei,^{62,48} H. Leithoff,²⁷ M. Lellmann,²⁷ T. Lenz,²⁷ C. Li,³⁸ C. H. Li,³¹ Cheng Li,^{62,48} D. M. Li,⁷⁰ F. Li,^{1,48} G. Li,¹ H. Li,⁴² H. Li,^{62,48} H. B. Li,^{1,53} H. J. Li,¹⁵ J. L. Li,⁴⁰ J. Q. Li,⁴ J. S. Li,⁴⁹ Ke Li,¹ L. K. Li,¹ Lei Li,³ P. R. Li,^{30,k,l} S. Y. Li,⁵¹ W. D. Li,^{1,53} W. G. Li,¹ X. H. Li,^{62,48} X. L. Li,⁴⁰ Xiaoyu Li,^{1,53} Z. Y. Li,⁴⁹ H. Liang,^{1,53} H. Liang,^{62,48} H. Liang,²⁶ Y. F. Liang,⁴⁴ Y. T. Liang,²⁴ G. R. Liao,¹² L. Z. Liao,^{1,53} J. Libby,²⁰ A. Limphirat,⁵⁰ C. X. Lin,⁴⁹ T. Lin,¹ B. J. Liu,¹ C. X. Liu,¹ D. Liu,^{14,62} F. H. Liu,⁴³ Fang Liu,¹ Feng Liu,⁶ H. M. Liu,^{1,53} Huanhuan Liu,¹ Huihui Liu,¹⁶ J. B. Liu,^{62,48} J. L. Liu,⁶³ J. Y. Liu,^{1,53} K. Liu,¹ K. Y. Liu,³² Ke Liu,⁶ L. Liu,^{62,48} M. H. Liu,^{9,f} P. L. Liu,¹ Q. Liu,⁶⁷ Q. Liu,⁵³ S. B. Liu,^{62,48} Shuai Liu,⁴⁵ T. Liu,^{9,f} T. Liu,^{1,53} W. M. Liu,^{62,48} X. Liu,^{30,k,l} Y. Liu,^{30,k,l} Y. B. Liu,³⁵ Z. A. Liu,^{1,48,53} Z. Q. Liu,⁴⁰ X. C. Lou,^{1,48,53} F. X. Lu,⁴⁹ H. J. Lu,¹⁷ J. D. Lu,^{1,53} J. G. Lu,^{1,48} X. L. Lu,¹ Y. Lu,¹ Y. P. Lu,^{1,48} C. L. Luo,³³ M. X. Luo,⁶⁹ P. W. Luo,⁴⁹ T. Luo,^{9,f} X. L. Luo,^{1,48} X. R. Lyu,⁵³ F. C. Ma,³² H. L. Ma,¹ L. L. Ma,⁴⁰ M. M. Ma,^{1,53} Q. M. Ma,¹ R. Q. Ma,^{1,53} R. T. Ma,⁵³ X. X. Ma,^{1,53} X. Y. Ma,^{1,48} F. E. Maas,¹⁴ M. Maggiora,^{65a,65c} S. Maldaner,⁴ S. Malde,⁶⁰ Q. A. Malik,⁶⁴ A. Mangoni,^{22b} Y. J. Mao,^{37,h} Z. P. Mao,¹ S. Marcello,^{65a,65c} Z. X. Meng,⁵⁶ J. G. Messchendorp,⁵⁴ G. Mezzadri,^{23a} T. J. Min,³⁴ R. E. Mitchell,²¹ X. H. Mo,^{1,48,53} N. Yu. Muchnoi,^{10,b} H. Muramatsu,⁵⁸ S. Nakhoul,^{11,d} Y. Nefedov,²⁸ F. Nerling,^{11,d} I. B. Nikolaev,^{10,b} Z. Ning,^{1,48} S. Nisar,^{8,g} S. L. Olsen,⁵³ Q. Ouyang,^{1,48,53} S. Pacetti,^{22b,22c} X. Pan,^{9,f} Y. Pan,⁵⁷ A. Pathak,¹ A. Pathak,²⁶ P. Patteri,^{22a} M. Pelizaeus,⁴ H. P. Peng,^{62,48} K. Peters,^{11,d} J. Pettersson,⁶⁶ J. L. Ping,³³ R. G. Ping,^{1,53} S. Pogodin,²⁸ R. Poling,⁵⁸ V. Prasad,^{62,48} H. Qi,^{62,48} H. R. Qi,⁵¹ K. H. Qi,²⁴ M. Qi,³⁴ T. Y. Qi,⁹ S. Qian,^{1,48} W. B. Qian,⁵³ Z. Qian,⁴⁹ C. F. Qiao,⁵³ L. Q. Qin,¹² X. P. Qin,⁹ X. S. Qin,⁴⁰ Z. H. Qin,^{1,48} J. F. Qiu,¹ S. Q. Qu,³⁵ K. H. Rashid,⁶⁴ K. Ravindran,²⁰ C. F. Redmer,²⁷ A. Rivetti,^{65c} V. Rodin,⁵⁴ M. Rolo,^{65c} G. Rong,^{1,53} Ch. Rosner,¹⁴ M. Rump,⁵⁹ H. S. Sang,⁶² A. Sarantsev,^{28,c} Y. Schelhaas,²⁷ C. Schnier,⁴ K. Schoenning,⁶⁶ M. Scodeggio,^{23a,23b} D. C. Shan,⁴⁵ W. Shan,¹⁸ X. Y. Shan,^{62,48} J. F. Shanguan,⁴⁵ M. Shao,^{62,48} C. P. Shen,⁹ H. F. Shen,^{1,53} P. X. Shen,³⁵ X. Y. Shen,^{1,53} H. C. Shi,^{62,48} R. S. Shi,^{1,53} X. Shi,^{1,48} X. D. Shi,^{62,48} J. J. Song,⁴⁰ W. M. Song,^{26,1} Y. X. Song,^{37,h} S. Sosio,^{65a,65c} S. Spataro,^{65a,65c} K. X. Su,⁶⁷ P. P. Su,⁴⁵ F. F. Sui,⁴⁰ G. X. Sun,¹ H. K. Sun,¹ J. F. Sun,¹⁵ L. Sun,⁶⁷ S. S. Sun,^{1,53} T. Sun,^{1,53} W. Y. Sun,²⁶ W. Y. Sun,³³ X. Sun,^{19,i} Y. J. Sun,^{62,48} Y. Z. Sun,¹ Z. T. Sun,¹ Y. H. Tan,⁶⁷ Y. X. Tan,^{62,48} C. J. Tang,⁴⁴ G. Y. Tang,¹ J. Tang,⁴⁹ J. X. Tang,^{62,48} V. Thoren,⁶⁶ W. H. Tian,⁴² Y. T. Tian,²⁴ I. Uman,^{52b} B. Wang,¹ C. W. Wang,³⁴ D. Y. Wang,^{37,h} H. J. Wang,^{30,k,l} H. P. Wang,^{1,53} K. Wang,^{1,48} L. L. Wang,¹ M. Wang,⁴⁰ M. Z. Wang,^{37,h} Meng Wang,^{1,53} S. Wang,^{9,f} W. Wang,⁴⁹ W. H. Wang,⁶⁷ W. P. Wang,^{62,48} X. Wang,^{37,h} X. F. Wang,^{30,k,l} X. L. Wang,^{9,f} Y. Wang,⁴⁹ Y. Wang,^{62,48} Y. D. Wang,³⁶ Y. F. Wang,^{1,48,53} Y. Q. Wang,¹ Y. Y. Wang,^{30,k,l} Z. Wang,^{1,48} Z. Y. Wang,¹ Ziyi Wang,⁵³ Zongyuan Wang,^{1,53} D. H. Wei,¹² F. Weidner,⁵⁹ S. P. Wen,¹ D. J. White,⁵⁷ U. Wiedner,⁴ G. Wilkinson,⁶⁰ M. Wolke,⁶⁶ L. Wollenberg,⁴ J. F. Wu,^{1,53} L. H. Wu,¹ L. J. Wu,^{1,53} X. Wu,^{9,f} Z. Wu,^{1,48} L. Xia,^{62,48} H. Xiao,^{9,f} S. Y. Xiao,¹ Z. J. Xiao,³³ X. H. Xie,^{37,h} Y. G. Xie,^{1,48} Y. H. Xie,⁶ T. Y. Xing,^{1,53} C. J. Xu,⁴⁹ G. F. Xu,¹ Q. J. Xu,¹³ W. Xu,^{1,53} X. P. Xu,⁴⁵ Y. C. Xu,⁵³ F. Yan,^{9,f} L. Yan,^{9,f} W. B. Yan,^{62,48} W. C. Yan,⁷⁰ Xu Yan,⁴⁵ H. J. Yang,^{41,e} H. X. Yang,¹ L. Yang,⁴² S. L. Yang,⁵³ Y. X. Yang,¹² Yifan Yang,^{1,53} Zhi Yang,²⁴ M. Ye,^{1,48} M. H. Ye,⁷ J. H. Yin,¹ Z. Y. You,⁴⁹ B. X. Yu,^{1,48,53} C. X. Yu,³⁵ G. Yu,^{1,53} J. S. Yu,^{19,i} T. Yu,⁶³ C. Z. Yuan,^{1,53} L. Yuan,² X. Q. Yuan,^{37,h} Y. Yuan,¹ Z. Y. Yuan,⁴⁹ C. X. Yue,³¹ A. A. Zafar,⁶⁴ X. Zeng Zeng,⁶ Y. Zeng,^{19,i} A. Q. Zhang,¹

B. X. Zhang,¹ Guangyi Zhang,¹⁵ H. Zhang,⁶² H. H. Zhang,²⁶ H. H. Zhang,⁴⁹ H. Y. Zhang,^{1,48} J. L. Zhang,⁶⁸ J. Q. Zhang,³³
 J. W. Zhang,^{1,48,53} J. Y. Zhang,¹ J. Z. Zhang,^{1,53} Jianyu Zhang,^{1,53} Jiawei Zhang,^{1,53} L. M. Zhang,⁵¹ L. Q. Zhang,⁴⁹
 Lei Zhang,³⁴ S. Zhang,⁴⁹ S. F. Zhang,³⁴ Shulei Zhang,^{19,i} X. D. Zhang,³⁶ X. Y. Zhang,⁴⁰ Y. Zhang,⁶⁰ Y. T. Zhang,⁷⁰
 Y. H. Zhang,^{1,48} Yan Zhang,^{62,48} Yao Zhang,¹ Z. Y. Zhang,⁶⁷ G. Zhao,¹ J. Zhao,³¹ J. Y. Zhao,^{1,53} J. Z. Zhao,^{1,48} Lei Zhao,^{62,48}
 Ling Zhao,¹ M. G. Zhao,³⁵ Q. Zhao,¹ S. J. Zhao,⁷⁰ Y. B. Zhao,^{1,48} Y. X. Zhao,²⁴ Z. G. Zhao,^{62,48} A. Zhemchugov,^{28,a}
 B. Zheng,⁶³ J. P. Zheng,^{1,48} Y. H. Zheng,⁵³ B. Zhong,³³ C. Zhong,⁶³ L. P. Zhou,^{1,53} Q. Zhou,^{1,53} X. Zhou,⁶⁷ X. K. Zhou,⁵³
 X. R. Zhou,^{62,48} X. Y. Zhou,³¹ A. N. Zhu,^{1,53} J. Zhu,³⁵ K. Zhu,¹ K. J. Zhu,^{1,48,53} S. H. Zhu,⁶¹ T. J. Zhu,⁶⁸ W. J. Zhu,^{9,f}
 W. J. Zhu,³⁵ Y. C. Zhu,^{62,48} Z. A. Zhu,^{1,53} B. S. Zou,¹ and J. H. Zou¹

(BESIII Collaboration)

¹*Institute of High Energy Physics, Beijing 100049, People's Republic of China*

²*Beihang University, Beijing 100191, People's Republic of China*

³*Beijing Institute of Petrochemical Technology, Beijing 102617, People's Republic of China*

⁴*Bochum Ruhr-University, D-44780 Bochum, Germany*

⁵*Carnegie Mellon University, Pittsburgh, Pennsylvania 15213, USA*

⁶*Central China Normal University, Wuhan 430079, People's Republic of China*

⁷*China Center of Advanced Science and Technology, Beijing 100190, People's Republic of China*

⁸*COMSATS University Islamabad, Lahore Campus, Defence Road, Off Raiwind Road,
54000 Lahore, Pakistan*

⁹*Fudan University, Shanghai 200443, People's Republic of China*

¹⁰*G.I. Budker Institute of Nuclear Physics SB RAS (BINP), Novosibirsk 630090, Russia*

¹¹*GSI Helmholtzcentre for Heavy Ion Research GmbH, D-64291 Darmstadt, Germany*

¹²*Guangxi Normal University, Guilin 541004, People's Republic of China*

¹³*Hangzhou Normal University, Hangzhou 310036, People's Republic of China*

¹⁴*Helmholtz Institute Mainz, Staudinger Weg 18, D-55099 Mainz, Germany*

¹⁵*Henan Normal University, Xixiang 453007, People's Republic of China*

¹⁶*Henan University of Science and Technology, Luoyang 471003, People's Republic of China*

¹⁷*Huangshan College, Huangshan 245000, People's Republic of China*

¹⁸*Hunan Normal University, Changsha 410081, People's Republic of China*

¹⁹*Hunan University, Changsha 410082, People's Republic of China*

²⁰*Indian Institute of Technology Madras, Chennai 600036, India*

²¹*Indiana University, Bloomington, Indiana 47405, USA*

^{22a}*INFN Laboratori Nazionali di Frascati, I-00044, Frascati, Italy*

^{22b}*INFN Sezione di Perugia, I-06100, Perugia, Italy*

^{22c}*University of Perugia, I-06100, Perugia, Italy*

^{23a}*INFN Sezione di Ferrara, I-44122, Ferrara, Italy*

^{23b}*University of Ferrara, I-44122, Ferrara, Italy*

²⁴*Institute of Modern Physics, Lanzhou 730000, People's Republic of China*

²⁵*Institute of Physics and Technology, Peace Avenue 54B, Ulaanbaatar 13330, Mongolia*

²⁶*Jilin University, Changchun 130012, People's Republic of China*

²⁷*Johannes Gutenberg University of Mainz, Johann-Joachim-Becher-Weg 45, D-55099 Mainz, Germany*

²⁸*Joint Institute for Nuclear Research, 141980 Dubna, Moscow region, Russia*

²⁹*Justus-Liebig-Universitaet Giessen, II. Physikalisches Institut,
Heinrich-Buff-Ring 16, D-35392 Giessen, Germany*

³⁰*Lanzhou University, Lanzhou 730000, People's Republic of China*

³¹*Liaoning Normal University, Dalian 116029, People's Republic of China*

³²*Liaoning University, Shenyang 110036, People's Republic of China*

³³*Nanjing Normal University, Nanjing 210023, People's Republic of China*

³⁴*Nanjing University, Nanjing 210093, People's Republic of China*

³⁵*Nankai University, Tianjin 300071, People's Republic of China*

³⁶*North China Electric Power University, Beijing 102206, People's Republic of China*

³⁷*Peking University, Beijing 100871, People's Republic of China*

³⁸*Qufu Normal University, Qufu 273165, People's Republic of China*

³⁹*Shandong Normal University, Jinan 250014, People's Republic of China*

⁴⁰*Shandong University, Jinan 250100, People's Republic of China*

⁴¹*Shanghai Jiao Tong University, Shanghai 200240, People's Republic of China*

⁴²*Shanxi Normal University, Linfen 041004, People's Republic of China*

⁴³*Shanxi University, Taiyuan 030006, People's Republic of China*

- ⁴⁴Sichuan University, Chengdu 610064, People's Republic of China
⁴⁵Soochow University, Suzhou 215006, People's Republic of China
⁴⁶South China Normal University, Guangzhou 510006, People's Republic of China
⁴⁷Southeast University, Nanjing 211100, People's Republic of China
⁴⁸State Key Laboratory of Particle Detection and Electronics, Beijing 100049, Hefei 230026, People's Republic of China
⁴⁹Sun Yat-Sen University, Guangzhou 510275, People's Republic of China
⁵⁰Suranaree University of Technology, University Avenue 111, Nakhon Ratchasima 30000, Thailand
⁵¹Tsinghua University, Beijing 100084, People's Republic of China
^{52a}Turkish Accelerator Center Particle Factory Group, Istinye University, 34010, Istanbul, Turkey
^{52b}Near East University, Nicosia, North Cyprus, Mersin 10, Turkey
⁵³University of Chinese Academy of Sciences, Beijing 100049, People's Republic of China
⁵⁴University of Groningen, NL-9747 AA Groningen, Netherlands
⁵⁵University of Hawaii, Honolulu, Hawaii 96822, USA
⁵⁶University of Jinan, Jinan 250022, People's Republic of China
⁵⁷University of Manchester, Oxford Road, Manchester, M13 9PL, United Kingdom
⁵⁸University of Minnesota, Minneapolis, Minnesota 55455, USA
⁵⁹University of Muenster, Wilhelm-Klemm-Str. 9, 48149 Muenster, Germany
⁶⁰University of Oxford, Keble Road, Oxford OX13RH, United Kingdom
⁶¹University of Science and Technology Liaoning, Anshan 114051, People's Republic of China
⁶²University of Science and Technology of China, Hefei 230026, People's Republic of China
⁶³University of South China, Hengyang 421001, People's Republic of China
⁶⁴University of the Punjab, Lahore-54590, Pakistan
^{65a}University of Turin and INFN, University of Turin, I-10125, Turin, Italy
^{65b}University of Eastern Piedmont, I-15121, Alessandria, Italy
^{65c}INFN, I-10125, Turin, Italy
⁶⁶Uppsala University, Box 516, SE-75120 Uppsala, Sweden
⁶⁷Wuhan University, Wuhan 430072, People's Republic of China
⁶⁸Xinyang Normal University, Xinyang 464000, People's Republic of China
⁶⁹Zhejiang University, Hangzhou 310027, People's Republic of China
⁷⁰Zhengzhou University, Zhengzhou 450001, People's Republic of China



(Received 14 October 2021; accepted 22 March 2022; published 19 April 2022)

A search for invisible decays of the Λ baryon is carried out in the process $J/\psi \rightarrow \Lambda \bar{\Lambda}$ based on $(1.0087 \pm 0.0044) \times 10^{10}$ J/ψ events collected with the BESIII detector located at the BEPCII storage ring. No signals are found for the invisible decays of Λ baryon, and the upper limit of the branching fraction is determined to be 7.4×10^{-5} at the 90% confidence level. This is the first search for invisible decays of baryons; such searches will play an important role in constraining dark sector models related to the baryon asymmetry.

DOI: 10.1103/PhysRevD.105.L071101

^aAlso at the Moscow Institute of Physics and Technology, Moscow 141700, Russia.

^bAlso at the Novosibirsk State University, Novosibirsk, 630090, Russia.

^cAlso at the NRC “Kurchatov Institute,” PNPI, 188300, Gatchina, Russia.

^dAlso at Goethe University Frankfurt, 60323 Frankfurt am Main, Germany.

^eAlso at Key Laboratory for Particle Physics, Astrophysics and Cosmology, Ministry of Education; Shanghai Key Laboratory for Particle Physics and Cosmology; Institute of Nuclear and Particle Physics, Shanghai 200240, People's Republic of China.

^fAlso at Key Laboratory of Nuclear Physics and Ion-beam Application (MOE) and Institute of Modern Physics, Fudan University, Shanghai 200443, People's Republic of China.

^gAlso at Harvard University, Department of Physics, Cambridge, Massachusetts 02138, USA.

^hAlso at State Key Laboratory of Nuclear Physics and Technology, Peking University, Beijing 100871, People's Republic of China.

ⁱAlso at School of Physics and Electronics, Hunan University, Changsha 410082, China.

^jAlso at Guangdong Provincial Key Laboratory of Nuclear Science, Institute of Quantum Matter, South China Normal University, Guangzhou 510006, China.

^kAlso at Frontiers Science Center for Rare Isotopes, Lanzhou University, Lanzhou 730000, People's Republic of China.

^lAlso at Lanzhou Center for Theoretical Physics, Lanzhou University, Lanzhou 730000, People's Republic of China.

Published by the American Physical Society under the terms of the [Creative Commons Attribution 4.0 International license](https://creativecommons.org/licenses/by/4.0/). Further distribution of this work must maintain attribution to the author(s) and the published article's title, journal citation, and DOI. Funded by SCOAP³.

Understanding dark matter is a highly topical subject in both astronomy and particle physics. Although strong indirect evidence for the existence of dark matter is obtained via astronomy, there is no direct evidence from collider experiments yet. On the other hand, the asymmetry between matter and antimatter in the Universe indicates that baryon number (B) conservation is violated [1]. The baryon matter density and the dark matter density are similar, $\rho_{\text{DM}} \approx 5.4\rho_{\text{baryon}}$, which may hint at a common origin of these two unsolved questions. Dark matter may be represented by baryon matter with invisible final state [2]. In the asymmetric dark matter scenario [3–8], the dark matter and baryon asymmetry puzzles may be related and the dark matter mass could be in the order of GeV. Simultaneous generation of the necessary baryon asymmetry and dark matter density is possible [9–11]. Those models usually contain a neutron portal operator $u^c d^c d^c$ [12,13], where q^c is the right-handed quark, to couple directly with dark matter or dark sector particles via effective operators obtained after integrating out a color-triplet scalar. Such operators can generally introduce B violation to the Standard Model sector. This type of interaction has been used to explain the discrepancy of neutron lifetime measurements in the beam method [14–17] and the bottle method [18–25], by requiring 1% of the neutrons to decay into dark matter particles [26]. Neutrons and antineutrons can also oscillate if the neutron portal couples to a Majorana dark sector particle, leading to a $\Delta B = 2$ process [27]. A mirror world with mirror dark matter can lead to a similar phenomenon [28,29]. Recently, exotic baryon number violating decays of hydrogen atoms to dark sector particles and neutrinos through the neutron portal have been discussed [30]. Moreover, allowing for quarks from the second and third generation in the neutron portal will generally result in new portals, which can lead to heavy flavor meson and baryon decays into dark sector particles. Specifically, b hadrons like $B_{d,s}^0$, B^\pm and Λ_b have been discussed [31,32]; their exotic decays could be probed at Belle II and in the LHC experiments. As many theories and experiments suggest a potential correlation between baryon symmetry and dark sector, study of baryon invisible decays is well motivated.

The search for invisible decays of neutral hadrons is highly interesting, since such decays could involve a potential dark matter candidate. Since the missing energy cannot be fully measured at hadron colliders [33], such studies are difficult to perform there. Electron-positron collision experiments such as BESIII and Belle II have the ability to probe invisible decays, benefiting from a well-defined production process and a clean reaction environment. Stringent limits on the invisible decays of Υ [34], J/ψ [35], B^0 [36], $\eta^{(\prime)}$ [37], π^0 [38], D^0 [39], ω [40], and ϕ [40] mesons have already been determined by several experiments. However, no experimental study of invisible baryon decays has been carried out yet. A search for

invisible decays of the Λ hyperon may provide information which can help to understand invisible decays of neutrons.

In this paper, the first experimental search for invisible decays of the Λ baryon is carried out using $(1.0087 \pm 0.0044) \times 10^{10}$ J/ψ events [41] accumulated at the center-of-mass energy $\sqrt{s} = 3.097$ GeV with the BESIII detector [42] at the BEPCII storage ring [43,44]. Taking advantage of the clean environment of $\Lambda\bar{\Lambda}$ pairs produced in $J/\psi \rightarrow \Lambda\bar{\Lambda}$, one $\bar{\Lambda}$ is explicitly reconstructed via $\bar{\Lambda} \rightarrow \bar{p}\pi^+$, allowing to search for invisible decays of the recoiling Λ . Invisible $\bar{\Lambda}$ decays are not pursued in this work, because the dominant background from $\bar{\Lambda} \rightarrow \bar{n}\pi^0$ is hard to estimate due to the difficulties in simulating the hadronic interactions of antineutrons with the detector material. An antineutron can induce a large number of showers spread over the detector, which introduces difficulties of finding a clean antineutron control sample to correct the Monte Carlo (MC) simulation.

The BESIII detector records symmetric e^+e^- collisions provided by the BEPCII storage ring. The cylindrical core of the BESIII detector covers nearly 93% of the full solid angle and consists of a helium-based multilayer drift chamber (MDC), a plastic scintillator time-of-flight system (TOF), and a CsI(Tl) electromagnetic calorimeter (EMC), which are all enclosed in a superconducting solenoidal magnet providing a 1.0 T (0.9 T in 2012) magnetic field. About 91% of the data was taken with the larger field. The solenoid is supported by an octagonal flux-return yoke with resistive plate counter muon identification modules interleaved with steel. The charged-particle momentum resolution at 1 GeV/ c is 0.5%. The EMC measures energies of photons with a resolution of 2.5% (5%) at 1 GeV in the barrel (end cap) region. The time resolution in the TOF barrel region is 68 ps, and it was 110 ps in the end cap region before 2015. An end cap TOF system upgrade in 2015 using multigap resistive plate chamber technology improved the time resolution to 60 ps [45] for about 87% of the dataset.

Simulated data samples produced with a GEANT4-based [46] MC package, which includes the geometric description and response of the detector, are used to determine the detection efficiency and understand background contributions. The simulation takes into account the beam energy spread and initial state radiation in the e^+e^- annihilations with the generator KKMC [47]. A sample of 1.0011×10^{10} simulated inclusive J/ψ decays is used. The inclusive MC sample includes both the production of the J/ψ resonance and the continuum processes incorporated in KKMC. The known decays are modelled with EVTGen [48] using branching fractions taken from the Particle Data Group [49]. The remaining unknown J/ψ decays are modelled with LundCharm [50]. Final state radiation of charged final state particles is incorporated using the PHOTOS package [51]. For the signal MC sample, the helicity formalism [52] is applied for $J/\psi \rightarrow \Lambda\bar{\Lambda}$ followed by the Λ decaying invisibly and the $\bar{\Lambda}$ decaying into $\bar{p}\pi^+$.

In the two-body decay of $J/\psi \rightarrow \Lambda \bar{\Lambda}$, the Λ can be inferred by detecting the $\bar{\Lambda}$ decay, which provides a model-independent way to study Λ decays without relying on the total number of J/ψ decays. In this philosophy, the number of events with a $\bar{\Lambda}$ detected is denoted as N_{tag} , and the number of events in which the signal decay of the accompanying Λ is also detected is denoted as N_{sig} . Therefore, the branching fraction for the signal decay is given as

$$\mathcal{B}(\Lambda \rightarrow \text{invisible}) = \frac{N_{\text{sig}}}{N_{\text{tag}} \cdot (\varepsilon_{\text{sig}}/\varepsilon_{\text{tag}})}. \quad (1)$$

Here, ε_{sig} is the detection efficiency when both $\bar{\Lambda}$ and Λ decays are selected and ε_{tag} is the efficiency of only detecting the $\bar{\Lambda}$ in $J/\psi \rightarrow \Lambda \bar{\Lambda}$. A semiblind analysis is performed to avoid possible bias, where 1% of the full data sample is used to validate the analysis strategy. The final results are obtained with the full data sample only after the analysis method is frozen.

To select $\bar{\Lambda}$ tag events, at least two charged particle tracks must be reconstructed in the MDC. They are required to have a polar angle θ with respect to the symmetry axis of the MDC satisfying $|\cos \theta| < 0.93$. Particle identification uses measurements of dE/dx in the MDC, forming likelihoods $\mathcal{L}(h)$ ($h = K, \pi, p$) for each hadron h hypothesis. The \bar{p} is identified by requiring $\mathcal{L}(\bar{p}) > \mathcal{L}(\pi^-)$ and $\mathcal{L}(\bar{p}) > \mathcal{L}(K^-)$. The π^+ is identified by requiring $\mathcal{L}(\pi^+) > \mathcal{L}(p)$ and $\mathcal{L}(\pi^+) > \mathcal{L}(K^+)$. At least one π^+ and one \bar{p} are required.

To reconstruct the $\bar{\Lambda}$, the $\bar{p}\pi^+$ tracks are constrained to a common vertex by applying a vertex fit, and the corresponding χ^2 is required to be less than 200. To further suppress background contributions, a constraint of the $\bar{\Lambda}$ momentum vector pointing to the interaction point is implemented and the corresponding χ^2 must be less than 10. The fitted decay length is required to be larger than three times its resolution. The updated momentum of the $\bar{p}\pi^+$ pairs after the constrained fit is used in the subsequent analysis. In addition, the cosine of the polar angle of the $\bar{\Lambda}$ candidate is required to be less than 0.70 to ensure that the Λ decay products are in the acceptance of the EMC barrel region which covers polar angles of $|\cos \theta| < 0.83$. To obtain a good resolution of the event start time and hence ensure that all the showers are in time with the event, one of the two charged tracks is required to leave cluster information in one of the TOF layers. The relative efficiency of this requirement is $(89.67 \pm 0.15)\%$. The invariant mass of $\bar{p}\pi^+$ is required to be within $5 \text{ MeV}/c^2$ of the nominal $\bar{\Lambda}$ mass. Those events with exactly one $\bar{\Lambda}$ candidate are retained for further studies.

The $\bar{\Lambda}$ single tag yield N_{tag} is obtained from a binned maximum likelihood fit to the recoil mass distribution $RM(\bar{p}\pi^+)$ as depicted in Fig. 1. In the fit, the signal

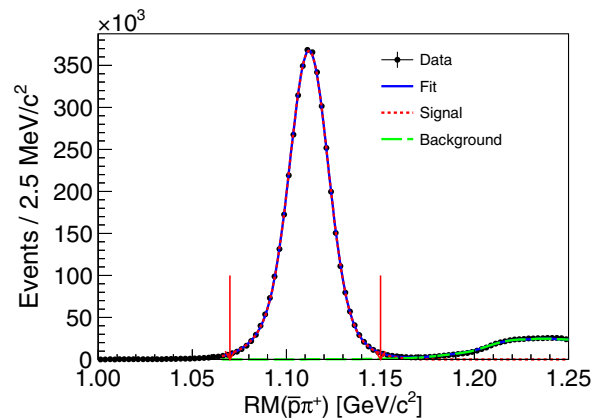


FIG. 1. Fit to the recoil mass of $\bar{p}\pi^+$. The black dots with uncertainties represent data and the blue solid line shows the total fit. The red curve and green long-dashed curve are the fitted signal and background contributions, respectively.

is modeled with a double Gaussian function, while background contributions are described with the shape derived from the inclusive MC sample. We find $N_{\text{tag}} = (4154428 \pm 2040)$ by integrating the signal function within $\pm 40 \text{ MeV}/c^2$ of the nominal Λ mass. The signal purity is 99.85% and the tagging efficiency is estimated to be $\varepsilon_{\text{tag}} = (32.11 \pm 0.01)\%$ based on a MC sample of $J/\psi \rightarrow \Lambda \bar{\Lambda}$ with $\bar{\Lambda} \rightarrow \bar{p}\pi^+$ and inclusive Λ decays.

To select signal candidates of the invisible Λ decays, $RM(\bar{p}\pi^+)$ is required to be within $40 \text{ MeV}/c^2$ of the nominal Λ mass. It is required that there is no additional charged track; this has a relative efficiency of $\varepsilon_{\text{sig}}/\varepsilon_{\text{tag}} = (94.64 \pm 0.17)\%$. The efficiency loss is mainly due to secondary tracks originating from the antiprotons interacting with the detector material. As the invisible Λ decay final states do not deposit any energy in the EMC, the sum of energies of all the EMC showers not associated with any charged tracks, E_{EMC} , can be used as a discriminator. Suppression of EMC showers from charged tracks is achieved by an isolation requirement: the angles between any shower included in the sum and the momenta of the π^+ and \bar{p} tracks must be greater than 10° and 20° , respectively.

As inferred from studies of the inclusive MC sample, $\Lambda \rightarrow n\pi^0$ is the dominant background after applying all selection conditions. However, due to the inaccurately modeled neutron interactions in the detector material by the GEANT4 package, the simulation of the energy deposits of neutrons in the EMC is unreliable, as illustrated in Fig. 2. Therefore, the MC-derived shape of this background contribution is corrected based on a neutron control sample, which can be used to model the energy deposit in the EMC from the penetrating neutron. The energy deposit in the EMC can be divided into three parts, as detailed below

$$E_{\text{EMC}} = E_{\text{EMC}}^{n^0} + E_{\text{EMC}}^n + E_{\text{EMC}}^{\text{noise}}, \quad (2)$$

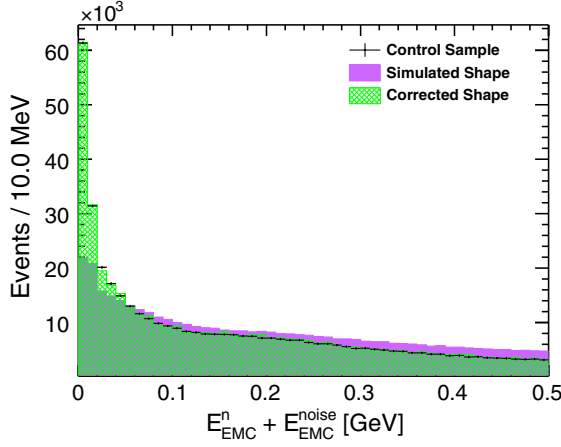


FIG. 2. The $E_{\text{EMC}}^n + E_{\text{EMC}}^{\text{noise}}$ distribution in $J/\psi \rightarrow \bar{p}\pi^+n$ control sample. Data points with error bars represent neutron control sample in data. The purple full filled histogram shows the GEANT4-based simulated shape, and the green cross filled histogram shows the corrected shape.

where $E_{\text{EMC}}^{\pi^0}$ is the energy due to electromagnetic showers from π^0 decays, E_{EMC}^n is the energy deposited by neutrons, and $E_{\text{EMC}}^{\text{noise}}$ is the energy of showers unrelated to the event. Among them, $E_{\text{EMC}}^{\pi^0}$ is retained based on MC simulations as the interactions of photons or electrons with material are reliably described in the simulation. The information of $E_{\text{EMC}}^{\pi^0}$ is recorded by switching off the interactions of \bar{p} , π^+ and n with the detector material in the exclusive simulation of the background process of $J/\psi \rightarrow \Lambda(n\pi^0)\bar{\Lambda}(\bar{p}\pi^+)$. For the sum of E_{EMC}^n and $E_{\text{EMC}}^{\text{noise}}$, a neutron control sample of $J/\psi \rightarrow \Lambda(n\pi^0)\bar{\Lambda}(\bar{p}\pi^+)$, $\pi^0 \rightarrow \gamma\gamma$ is selected, where all final state particles are detected except the neutron. A series of shape templates as a function of the momentum and polar angle of the neutron is derived by summing up the energies of all the showers except the photon showers from π^0 decays, which are not associated with the $\bar{p}\pi^+$ tracks. The corrected E_{EMC} shape for $\Lambda \rightarrow n\pi^0$ background contributions is derived by combining $E_{\text{EMC}}^{\pi^0}$ with a random value of the sum of E_{EMC}^n and $E_{\text{EMC}}^{\text{noise}}$ from the shape template according to the momentum and polar angle of the neutron in the exclusive MC simulations. The above mentioned correction procedure has been validated based on the control sample of $J/\psi \rightarrow p\bar{p}\pi^0$ and $\bar{p}\pi^+n$, where $p\bar{p}\pi^0$ is used to check the π^0 simulation and $\bar{p}\pi^+n$ to cross check the two-dimensional resampling method on the EMC shower energy of the neutron control sample. Figure 2 shows that the resampled shape of $E_{\text{EMC}}^n + E_{\text{EMC}}^{\text{noise}}$ well reproduce the original shape in $J/\psi \rightarrow \bar{p}\pi^+n$ control sample.

The corrected distribution of E_{EMC} is shown in Fig. 3, where the resulting E_{EMC} distribution for the $\Lambda \rightarrow n\pi^0$ background and for other remaining minor Λ decay background contributions, such as $\Lambda \rightarrow n\gamma$ with size of 0.5% of

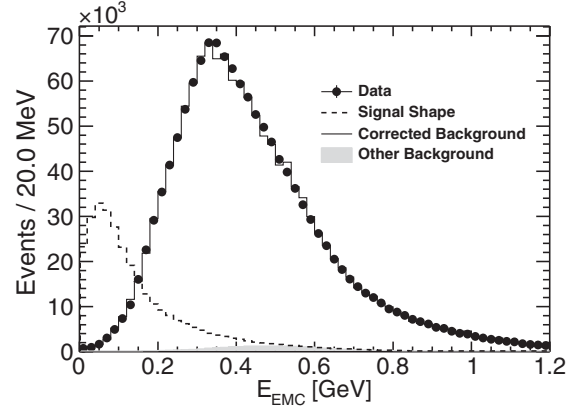


FIG. 3. The E_{EMC} distribution. The dots with uncertainties represent data. The dashed line shows the signal shape, where the corresponding yield is normalized arbitrarily for clarity. The solid line shows the $\Lambda \rightarrow n\pi^0$ background shape including the correction. The grey filled area shows the other background contributions mentioned in the text.

$\Lambda \rightarrow n\pi^0$ background, in the inclusive MC sample is overlaid. The signal of invisible Λ decays is expected to peak close to zero, as the dashed line in Fig. 3 shows. The signal shape can be modeled by MC simulations from noise plus a small contribution from charged-particle showers leaking through the isolation requirement.

The total E_{EMC} distribution from the simulated J/ψ decay background is found to agree well with the data, no obvious signal is observed. An upper limit (UL) at 90% confidence level (C.L.) on the branching fraction of invisible Λ decays, $\mathcal{B}(\Lambda \rightarrow \text{invisible})$, is evaluated by a binned maximum likelihood fit to the E_{EMC} distribution, after taking into account the effects of statistical and systematic uncertainties. Here, the number of signal events N_{sig} is obtained by integrating the signal fraction of the fit function.

The systematic uncertainties on $\mathcal{B}(\Lambda \rightarrow \text{invisible})$ due to the selection criteria used for tagging $\bar{\Lambda}$ candidates cancel in Eq. (1). The systematic uncertainty related to the determination of N_{tag} is found to be negligible. The sources of the dominant systematic uncertainties are the selection condition regarding the separation angle between the EMC shower and the anti-proton, the choice of binning in fitting to the E_{EMC} distributions and the requirement of no additional charged track. In the former two cases, we vary the condition (the binning) as summarized in Table I.

Antiproton interactions with the EMC material can produce a large number of fake photon signals over a large area. The requirement on the opening angle between the shower direction and the \bar{p} track extrapolated to the EMC can affect the E_{EMC} shape in both signal and background processes. To take this effect into account, different choices of separation angles are tested in the analysis procedure. In the likelihood fit, five different

TABLE I. Sources of systematic uncertainties, which are taken into account in estimating the UL of the invisible Λ decay rate.

Source	Choice or uncertainty
Shower separation angle	18°, 20° and 22°
Bin width	10, 20, 30, 40, 50 MeV
No additional charged track	0.6%

choices of bin widths are considered with a minimum width of 10 MeV. The requirement of no additional charged tracks affects the estimation of the detection efficiency and the E_{EMC} distribution. To study this systematic effect, a clean control sample of $J/\psi \rightarrow \Lambda(p\pi^-)\bar{\Lambda}(\bar{p}\pi^+)$ is selected requiring a full detection of all final state charged tracks. The efficiency difference of the further requirement of no additional charged tracks between data and MC simulations is found to be 0.6%.

A modified frequentist approach [53,54], which incorporates all the systematic and statistical uncertainties, is adopted to estimate the UL of $\mathcal{B}(\Lambda \rightarrow \text{invisible})$. In the procedure, thousands of pseudodata samples are generated according to the E_{EMC} distributions in data. In each sample, the number of events is randomly chosen with a Poisson distribution with a mean value corresponding to the data. This approach incorporates the statistical fluctuation. A binned maximum likelihood fit is implemented, where the signal model is taken from the signal MC sample, and $\Lambda \rightarrow n\pi^0$ background contributions are described with the MC-determined shape after correction with the neutron control sample. The sizes of these two components are free parameters in each fit. The size and shape of the remaining Λ decay backgrounds are fixed according to the inclusive MC sample; this is found to cause negligible uncertainty. Values of bin width and the shower separation angle, as listed in Table I, are randomly selected and applied to the corresponding signal and background models. To calculate $\mathcal{B}(\Lambda \rightarrow \text{invisible})$, the involved efficiency ratio $\varepsilon_{\text{sig}}/\varepsilon_{\text{tag}}$ in

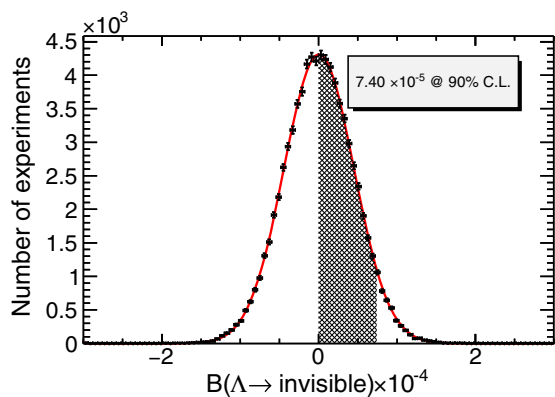


FIG. 4. Distribution of the estimated $\mathcal{B}(\Lambda \rightarrow \text{invisible})$ in pseudosamples. The shaded area corresponds to the 90% coverage in the physical region.

Eq. (1) is scaled with a factor randomly sampled from a Gaussian function with mean of 1 and width of 0.006. The resulting distribution of the calculated branching fractions in the pseudosamples is shown in Fig. 4, described by a Gaussian function. The UL on $\mathcal{B}(\Lambda \rightarrow \text{invisible})$ at 90% C.L. is determined by integrating in the physical region ($\mathcal{B} > 0$). The corresponding UL is obtained to be 7.4×10^{-5} , including the systematic uncertainties.

In summary, with a sample of $(1.0087 \pm 0.0044) \times 10^{10}$ J/ψ events collected by the BESIII detector, the first search for invisible decays of the Λ hyperon is carried out. This is the first direct experimental search for invisible decays of baryons. No obvious signal is observed and the UL on the decay rate is $\mathcal{B}(\Lambda \rightarrow \text{invisible}) < 7.4 \times 10^{-5}$ at 90% C.L., which is consistent with the prediction of 4.4×10^{-7} from the mirror model [29]. This result sheds light on the neutron lifetime measurement puzzle [14–25] and helps to constrain dark sector models related to the baryon asymmetry.

The BESIII collaboration thanks the staff of BEPCII and the IHEP computing center for their strong support. We thank Yi Liao, Jia Liu and Fu-Sheng Yu for useful discussions. This work is supported in part by National Key Research and Development Program of China under Contracts No. 2020YFA0406400 and No. 2020YFA0406300; National Natural Science Foundation of China (NSFC) under Contracts No. 11625523, No. 11635010, No. 11735014, No. 11822506, No. 11835012, No. 11935015, No. 11935016, No. 11935018, No. 11961141012, No. 12022510, No. 12025502, No. 12035009, No. 12035013 and No. 12061131003; the Chinese Academy of Sciences (CAS) Large-Scale Scientific Facility Program; Joint Large-Scale Scientific Facility Funds of the NSFC and CAS under Contracts No. U1732263 and No. U1832207; CAS Key Research Program of Frontier Sciences under Contract No. QYZDJ-SSW-SLH040; 100 Talents Program of CAS; INPAC and Shanghai Key Laboratory for Particle Physics and Cosmology; ERC under Contract No. 758462; European Union Horizon 2020 research and innovation programme under Contract No. Marie Skłodowska-Curie Grant Agreement No. 894790; German Research Foundation DFG under Contract No. 443159800, Collaborative Research Center CRC 1044, FOR 2359, GRK 214; Istituto Nazionale di Fisica Nucleare, Italy; Ministry of Development of Turkey under Contract No. DPT2006K-120470; National Science and Technology fund; Olle Engkvist Foundation under Contract No. 200-0605; STFC (United Kingdom); The Knut and Alice Wallenberg Foundation (Sweden) under Contract No. 2016.0157; The Royal Society, UK under Contracts No. DH140054 and No. DH160214; The Swedish Research Council; U.S. Department of Energy under Contracts No. DE-FG02-05ER41374 and No. DE-SC-0012069.

- [1] A. D. Sakharov, Pis'ma Zh. Eksp. Teor. Fiz. **5**, 32 (1967) [JETP Lett. **5**, 24 (1967)] [Sov. Phys. Usp. **34**, 392 (1991)] [Usp. Fiz. Nauk **161**, 61 (1991)].
- [2] G. Alonso-Álvarez, G. Elor, M. Escudero, B. Fornal, B. Grinstein, and J. M. Camalich, arXiv:2111.12712.
- [3] S. Nussinov, Phys. Lett. **165B**, 55 (1985).
- [4] S. Dodelson and L. M. Widrow, Phys. Rev. D **42**, 326 (1990).
- [5] S. M. Barr, R. S. Chivukula, and E. Farhi, Phys. Lett. B **241**, 387 (1990).
- [6] D. B. Kaplan, Phys. Rev. Lett. **68**, 741 (1992).
- [7] G. R. Farrar and G. Zaharijas, Phys. Rev. Lett. **96**, 041302 (2006).
- [8] D. E. Kaplan, M. A. Luty, and K. M. Zurek, Phys. Rev. D **79**, 115016 (2009).
- [9] J. Shelton and K. M. Zurek, Phys. Rev. D **82**, 123512 (2010).
- [10] H. Davoudiasl, D. E. Morrissey, K. Sigurdson, and S. Tulin, Phys. Rev. Lett. **105**, 211304 (2010).
- [11] P. H. Gu, M. Lindner, U. Sarkar, and X. Zhang, Phys. Rev. D **83**, 055008 (2011).
- [12] K. Petraki and R. R. Volkas, Int. J. Mod. Phys. A **28**, 1330028 (2013).
- [13] K. M. Zurek, Phys. Rep. **537**, 91 (2014).
- [14] L. N. Bondarenko, V. V. Kurguzov, Y. A. Prokofev, E. V. Rogov, and P. E. Spivak, Pis'ma Zh. Eksp. Teor. Fiz. **28**, 328 (1978), <https://inspirehep.net/literature/135939>.
- [15] J. Byrne and P. G. Dawber, Europhys. Lett. **33**, 187 (1996).
- [16] L. Bottyan, D. G. Merkel, B. Nagy, and J. Major, Neutron News **23**, 21 (2012).
- [17] A. T. Yue, M. S. Dewey, D. M. Gilliam, G. L. Greene, A. B. Laptev, J. S. Nico, W. M. Snow, and F. E. Wietfeldt, Phys. Rev. Lett. **111**, 222501 (2013).
- [18] W. Mampe, L. N. Bondarenko, V. I. Morozov, Y. N. Panin, and A. I. Fomin, JETP Lett. **57**, 82 (1993), <https://inspirehep.net/literature/362243>.
- [19] A. Serebrov, V. Varlamov, A. Kharitonov, A. Fomin, Y. Pokotilovski, P. Geltenbort, J. Butterworth, I. Krasnoschekova, M. Lasakov, and R. Tal'daev *et al.*, Phys. Lett. B **605**, 72 (2005).
- [20] A. Pichlmaier, V. Varlamov, K. Schreckenbach, and P. Geltenbort, Phys. Lett. B **693**, 221–226 (2010).
- [21] A. Steyerl, J. M. Pendlebury, C. Kaufman, S. S. Malik, and A. M. Desai, Phys. Rev. C **85**, 065503 (2012).
- [22] S. Arzumanov, L. Bondarenko, S. Chernyavsky, P. Geltenbort, V. Morozov, V. V. Nesvizhevsky, Y. Panin, and A. Strepetov, Phys. Lett. B **745**, 79 (2015).
- [23] A. P. Serebrov, E. A. Kolomensky, A. K. Fomin, I. A. Krasnoschekova, A. V. Vassiljev, D. M. Prudnikov, I. V. Shoka, A. V. Chechkin, M. E. Chaikovskiy, and V. E. Varlamov *et al.*, Phys. Rev. C **97**, 055503 (2018).
- [24] R. W. Pattie, Jr., N. B. Callahan, C. Cude-Woods, E. R. Adamek, L. J. Broussard, S. M. Clayton, S. A. Currie, E. B. Dees, X. Ding, E. M. Engel *et al.*, Science **360**, 627 (2018).
- [25] V. F. Ezhov, A. Z. Andreev, G. Ban, B. A. Bazarov, P. Geltenbort, A. G. Glushkov, V. A. Knyazkov, N. A. Kovrizhnykh, G. B. Krygin, and O. Naviliat-Cuncic *et al.*, JETP Lett. **107**, 671 (2018).
- [26] B. Fornal and B. Grinstein, Phys. Rev. Lett. **120**, 191801 (2018); **124**, 219901(E) (2020).
- [27] D. G. Phillips II, W. M. Snow, K. Babu, S. Banerjee, D. V. Baxter, Z. Berezhiani, M. Bergevin, S. Bhattacharya, G. Brooijmans, and L. Castellanos *et al.*, Phys. Rep. **612**, 1 (2016).
- [28] W. Tan, Phys. Lett. B **797**, 134921 (2019).
- [29] W. Tan, arXiv:2006.10746.
- [30] D. McKeen, M. Pospelov, and N. Raj, Phys. Rev. Lett. **125**, 231803 (2020).
- [31] G. Alonso-Álvarez, G. Elor, and M. Escudero, Phys. Rev. D **104**, 035028 (2021).
- [32] G. Elor, M. Escudero, and A. Nelson, Phys. Rev. D **99**, 035031 (2019).
- [33] M. Borsato *et al.*, Rep. Prog. Phys. **85**, 024201 (2022).
- [34] B. Aubert *et al.* (BABAR Collaboration), Phys. Rev. Lett. **103**, 251801 (2009).
- [35] M. Ablikim *et al.* (BES Collaboration), Phys. Rev. Lett. **100**, 192001 (2008).
- [36] C. L. Hsu *et al.* (Belle Collaboration), Phys. Rev. D **86**, 032002 (2012).
- [37] M. Ablikim *et al.* (BESIII Collaboration), Phys. Rev. D **87**, 012009 (2013).
- [38] E. Cortina Gil *et al.* (NA62 Collaboration), J. High Energy Phys. **02** (2021) 201.
- [39] Y. T. Lai *et al.* (Belle Collaboration), Phys. Rev. D **95**, 011102 (2017).
- [40] M. Ablikim *et al.* (BESIII Collaboration), Phys. Rev. D **98**, 032001 (2018).
- [41] M. Ablikim *et al.* (BESIII Collaboration), Phys. Rev. D **103**, 112007 (2021).
- [42] M. Ablikim *et al.* (BESIII Collaboration), Nucl. Instrum. Methods Phys. Res., Sect. A **614**, 345 (2010).
- [43] C. H. Yu *et al.*, BEPCII Performance and Beam Dynamics Studies on Luminosity, in *Proceedings of IPAC2016, Busan, Korea* (JACoW, Geneva, Switzerland, 2016), 10.18429/JACoW-IPAC2016-TUYA01.
- [44] M. Ablikim *et al.* (BESIII Collaboration), Chin. Phys. C **44**, 040001 (2020).
- [45] X. Li *et al.*, Radiat. Detect. Technol. Methods **1**, 13 (2017); Y. X. Guo *et al.*, Radiat. Detect. Technol. Methods **1**, 15 (2017); P. Cao *et al.*, Nucl. Instrum. Methods Phys. Res., Sect. A **953**, 163053 (2020).
- [46] S. Agostinelli *et al.* (GEANT4 Collaboration), Nucl. Instrum. Methods Phys. Res., Sect. A **506**, 250 (2003).
- [47] S. Jadach, B. F. L. Ward, and Z. Was, Phys. Rev. D **63**, 113009 (2001); Comput. Phys. Commun. **130**, 260 (2000).
- [48] D. J. Lange, Nucl. Instrum. Methods Phys. Res., Sect. A **462**, 152 (2001); R. G. Ping, Chin. Phys. C **32**, 599 (2008).
- [49] P. A. Zyla *et al.* (Particle Data Group Collaboration), Prog. Theor. Exp. Phys. **2020**, 083C01 (2020).
- [50] J. C. Chen, G. S. Huang, X. R. Qi, D. H. Zhang, and Y. S. Zhu, Phys. Rev. D **62**, 034003 (2000); R. L. Yang, R. G. Ping, and H. Chen, Chin. Phys. Lett. **31**, 061301 (2014).
- [51] E. Richter-Was, Phys. Lett. B **303**, 163 (1993).
- [52] M. Ablikim *et al.* (BESIII Collaboration), Nat. Phys. **15**, 631 (2019).
- [53] M. Ablikim *et al.* (BESIII Collaboration), Phys. Rev. D **91**, 112015 (2015).
- [54] M. Ablikim *et al.* (BESIII Collaboration), Phys. Rev. D **95**, 071102 (2017).